Available online at www.sciencedirect.com

SCIENCE DIRECT®

ELSEVIER

Palaeogeography, Palaeoclimatology, Palaeoecology 223 (2005) 127–146

PALAEO

www.elsevier.com/locate/palaeo

Oxygen and hydrogen isotope compositions of Permian pedogenic phyllosilicates: Development of modern surface domain arrays and implications for paleotemperature reconstructions

Neil J. Tabor[a,*], Isabel P. Montañez[b]

[a]Department of Geosciences, Southern Methodist University, Dedman College, Dallas, TX 75275-0395, USA
[b]Department of Geology, University of California, One Shields Avenue, Davis, CA 95616, USA

Received 26 April 2004; received in revised form 4 March 2005; accepted 30 March 2005

Abstract

Mineralogic, chemical, and oxygen and hydrogen isotope compositions of 15 different phyllosilicate samples from Permo–Pennsylvanian-age paleosols of the eastern shelf of the Midland basin of Texas and the southern Anadarko basin are presented. Mixtures of 2 : 1 phyllosilicates and kaolinite dominate most samples, although some samples consist of relatively pure 2 : 1 phyllosilicates. Chemical and mineralogic data are used in conjunction with published thermodynamic data to calculate hydrogen and oxygen isotope fractionation factors for each sample. In turn, application of measured oxygen and hydrogen isotope compositions of the phyllosilicates to temperature-dependent fractionation equations are used to calculate paleotemperatures of crystallization.

The δD values of the phyllosilicates range from -69‰ to -55‰. The δ^{18}O values range from 19.5‰ to 22.7‰. If these samples preserve a record of equilibrium with paleo-meteoric waters, the isotopic compositions of the phyllosilicates correspond to paleotemperatures of phyllosilicate crystallization ranging from 22 ± 3 °C to 35 ± 3 °C. In particular, the stratigraphic trend of calculated temperatures from Midland basin samples suggests that Early Permian surface temperatures may have been up to 10 °C warmer than those of the latest Pennsylvanian.

Keywords: Oxygen and hydrogen isotopes of phyllosilicates; Paleotemperatures; Modern surface domains; Paleosols; Greenhouse climates

1. Introduction

Climate plays an important role in the deposition and distribution of many terrestrial lithologies such as coals, laterites, kaolins, red beds, calcretes, and eolianites (e.g., Parrish, 1993; Sellwood and Price, 1993; Ziegler et al., 1996; Barron and Moore, 1994). As

* Corresponding author. Fax: +1 214 768 2701.
E-mail address: ntabor@mail.smu.edu (N.J. Tabor).

0031-0182/$ - see front matter © 2005 Elsevier B.V. All rights reserved.
doi:10.1016/j.palaeo.2005.04.009

such, the terrestrial sedimentary record provides insight into the evolution of climate through the Phanerozoic. However, temperature, which is an integral component of climate and a strong influence on the distribution of climate zones, is poorly approximated by the character and morphology of terrestrial lithologies (e.g., Parrish, 1993). One potential quantitative proxy of paleotemperature is combined oxygen and hydrogen isotope ratios of ancient soil-formed (hereafter pedogenic) hydroxyl-bearing minerals. The potential of the isotopic compositions of these minerals to provide paleotemperature estimates is particularly attractive given their widespread occurrence in soils. In this regard, paleothermometry could be broadly applied to pedogenic systems of any age.

The potential utility of pedogenic phyllosilicates as isotopic archives of paleoenvironmental conditions and paleotemperature has been recognized since the early work of Savin and Epstein (1970). More recent work has demonstrated that combined study of the oxygen and hydrogen isotopic composition of hydroxyl-bearing minerals from pedogenic environments can yield more environmental information than either $\delta^{18}O$ or δD values alone (Yapp, 1987, 1993, 2000; Delgado and Reyes, 1996; Savin and Hsieh, 1998; Vitali et al., 2002). With few notable exceptions, this approach has seldom been applied in isotopic studies of phyllosilicate minerals (Bird and Chivas, 1988; 1989; Lawrence and Rashkes-Meaux, 1993; Vitali et al., 2002). These studies elucidate the challenge in isotopic analysis of pedogenic phyllosilicates in which (1) mixtures of authigenic and detrital minerals were analyzed together and end-member isotope compositions of the authigenic phases were calculated assuming the abundance and isotopic composition of the detrital phase, or (2) chemical variability among phyllosilicate samples, and attendant variability of the oxygen and hydrogen isotope fractionation factors associated with it, were largely unknown or ignored.

Although soils with pedogenic 2 : 1 phyllosilicate minerals are geographically and geologically more abundant than kaolinite-rich weathering profiles (e.g., Wilson, 1999), very few studies have applied combined oxygen and hydrogen isotopic studies of these minerals to paleoclimate and paleotemperature reconstructions (Delgado and Reyes, 1996; Vitali et al., 2002; Tabor et al., 2004). This primarily reflects the variable chemistry of 2 : 1 phyllosilicates, and the corresponding variability of thermodynamic isotopic fractionation factors for these minerals, relative to chemically invariant minerals such as kaolinite.

Based on profile-scale mineralogic analysis of the clay-size fraction (<2 μm) of the Permo–Pennsylvanian weathering profiles, Tabor et al. (2002) asserted that those paleosols preserve profile-scale mineralogic trends in phyllosilicate composition and abundance that are similar to modern pedogenic signatures and therefore isotopic compositions of the soil-formed minerals may have paleoenvironmental significance. This paper builds on the earlier work of Tabor et al. (2002) by presenting combined oxygen and hydrogen isotope compositions of paleopedogenic 2 : 1 phyllosilicates and kaolinite from 15 Permo–Pennsylvanian paleosol profiles that formed in the Eastern Shelf of the Midland basin (herein referred to as Eastern Midland basin) of Texas and the Anadarko basin of Oklahoma. Utilizing the concept of surface domain arrays defined by Yapp (1993, 2000), we assert that these paleopedogenic phyllosilicates preserve isotopic compositions similar to those expected in modern soil forming environments. These data provide new constraints that help to refine our understanding of Late Paleozoic climate and the role that climate may have played in the terrestrial sedimentary record.

1.1. Sample set and previous work

The stratigraphic distribution and geographic location of the samples are presented in Table 1. Fossil soils (paleosols) include Late Pennsylvanian (Virgilian) and Early Permian (Wolfcampian and Leonardian) examples from the Eastern Midland basin and Early Permian (Wolfcampian and Leonardian) samples from the extreme southern rim of the Anadarko basin in south-central Oklahoma. Chronostratigraphic constraints for all sections include fluvial marker beds and correlated marine limestones with good fusilinid and ammonite biostratigraphic control (Dunbar, 1960; Hentz, 1988; Donovan, 1986).

The Permo–Pennsylvanian strata of the Eastern Midland and Anadarko basins were deposited along the western coastal zone of equatorial Pangea (Ziegler et al., 1996; Golonka et al., 1994; Scotese, 1984; Loope et al., 2004). Major tectonic elements that influenced Late Paleozoic sedimentation within these two basins, such as the Muenster Arch and the

Table 1
Results of chemical and X-ray diffraction analyses of <0.2 μm-size fraction phyllosilicates[a]

Sample[b]	Series	Stage	Formation	Depth (m)[d]	Na_2O	MgO	Al_2O_3	SiO_2	P_2O_5	K_2O	CaO	TiO_2	Fe_2O_3	Total	Mineralogy[e]
Texas															
12	Permian	Leonardian	Clear Fork	710	2.42	3.49	28.71	54.60	0.03	4.53	0.01	0.30	5.37	99.47	Sm, HIM, K
11	Permian	Leonardian	Waggoner Ranch	620	4.60	4.01	26.25	56.82	0.02	1.87	0.03	0.58	5.96	100.14	Sm, HIM
10	Permian	Leonardian	Petrolia	525	5.93	3.68	28.91	55.82	0.02	0.81	0.05	0.46	4.86	100.53	Sm
9	Permian	Leonardian	Petrolia	475	2.74	2.84	29.58	55.22	0.03	3.08	0.02	0.41	5.27	99.18	Sm
8[c]	Permian	Wolfcampian	Nocona	415	2.94	4.18	26.82	57.34	B.D.	2.98	0.04	0.07	5.73	100.11	Sm, HIM, K
7	Permian	Wolfcampian	Nocona	395	2.24	2.50	29.34	55.41	0.03	2.06	0.03	0.79	7.38	99.78	Sm, K
6	Permian	Wolfcampian	Nocona	365	2.78	2.54	29.35	55.04	0.04	3.56	0.02	0.56	5.49	99.39	Sm, K, ML
5	Permian	Wolfcampian	Archer City	315	2.85	2.43	29.73	53.90	0.03	3.35	0.02	0.87	4.917	98.11	Sm, K
4	Permian	Wolfcampian	Archer City	265	6.88	1.90	30.99	56.16	0.02	0.76	0.03	0.36	3.82	100.92	Sm, HIM
3[c]	Permian	Wolfcampian	Archer City	230	1.63	2.89	29.35	57.24	B.D.	4.28	B.D.	0.23	4.28	99.9	Sm, K
MM3C	Pennsylvanian	Virgillian	Markley	205	1.20	2.68	24.83	56.60	0.04	4.33	0.03	0.87	7.71	98.28	Sm, HIM, ML
2	Pennsylvanian	Virgillian	Markley	180	0.79	0.82	36.83	54.17	0.06	1.66	0.09	0.73	2.73	97.88	K
1	Pennsylvanian	Virgillian	Markley	135	0.66	0.58	31.39	62.65	0.03	1.66	0.06	0.97	1.94	99.94	K, HIM
Oklahoma															
349941	Permian	Leonardian	Hennessey		0.36	2.63	31.72	56.32	0.02	2.69	0.03	0.38	4.69	98.83	Sm, K
Waur4a	Permian	Leonardian	Wellington		0.21	2.23	30.53	57.75	0.07	2.26	0.04	0.61	4.96	98.65	Sm, K, ML

[a] Chemical data are presented as the mean of 15 individual analyses for each sample.
[b] The mineralogical, elemental, and oxygen isotope values given for samples numbered 1 through 12 correspond to samples that are presented in Tabor et al. (2002). All of other samples, as well as all of the hydrogen isotope data, are presented for the first time here (i.e., only three new samples are introduced here).
[c] The chemical compositions of these samples differs from those reported in Tabor et al. (2002) because earlier analyses apparently were contaminated by excess sodium from 2 M NaCl treatment prior to chemical analysis. These samples were washed with DI H_2O 6 times and reanalyzed. The results of the new chemical analyses are reported here.
[d] Depths correspond to the approximate stratigraphic level of samples above the base of the Pennsylvanian Markley Formation in the Eastern Midland Basin of northern Texas.
[e] Representative X-Ray diffraction patterns as well as detailed descriptions and interpretations of mineralogical data for samples 1 through 12 are given in Tabor et al. (2002). The same approach to mineralogical and chemical analysis and interpretation of results that was used in Tabor et al. (2002) was applied to the new samples introduced here. Sm = smectite, K = kaolinite, HIM = hydroxy-interlayered material, ML = Mica-like mineral.

Wichita, Arbuckle and Ouachita Mountains, developed in latest Pennsylvanian time as a result of Pangean assembly and were essentially quiescent by Permian time (Oriel et al., 1967).

The Late Pennsylvanian and Permian strata of the Eastern Midland basin consist of alluvial mudrocks and sandstones that were deposited on a low-sloping shelf (>0.5°; e.g., Hentz, 1988). These strata are approximately 1250 m thick in the western study area and progressively thin eastward toward the Ouachita highlands (Fig 1; Hentz, 1988; Nelson et al., 2001; Tabor and Montañez, 2004). Cretaceous strata were probably deposited in the area, as indicated by Cretaceous marine outliers in the extreme western portions of the study area, but did not likely accumulate to a thickness of more than 330 m (Barnes et al., 1987). Tertiary and early Quaternary burial was insignificant in the study region (Barnes et al., 1987). Therefore, the maximum burial depth of the base of the studied stratigraphic succession in the Eastern Midland basin did not likely exceed 1600 m. This shallow burial history is reflected by burial tempera-

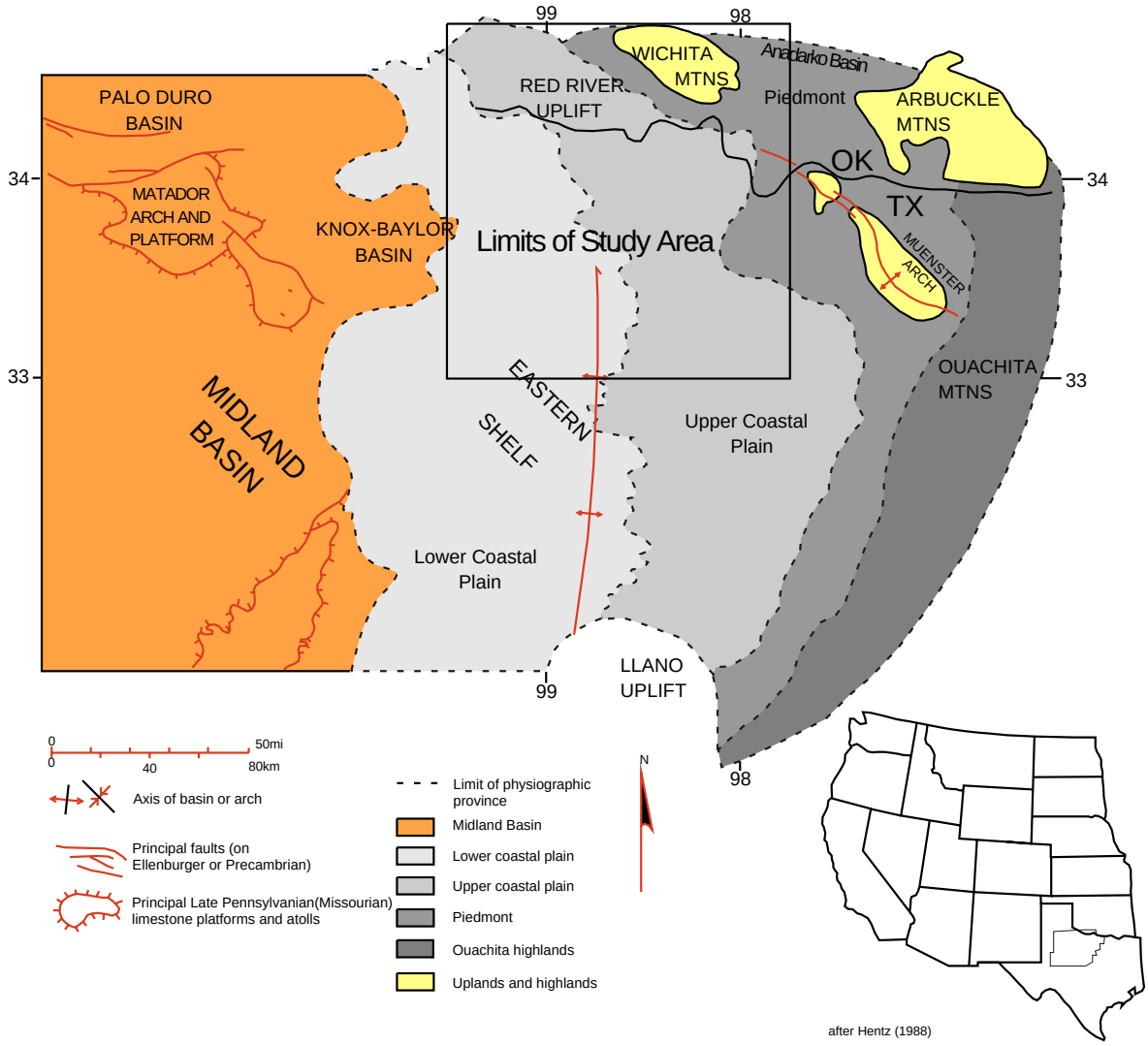

Fig. 1. Regional distribution of source terranes and physiographic provinces across the latest Pennsylvanian through early Permian landscape of the Eastern Shelf of the Midland basin, Texas and southern margin of the Anadarko basin, Oklahoma, U.S.A. Province boundaries are defined for the period of maximum regression in the earliest Permian. Structural and tectonic elements shown are for the pre-Virgilian paleogeography of north-central Texas; the Muenster and Ouachita highlands remained significant topographic features in the Early Permian. Diagram modified after Hentz (1988).

tures estimated to have never exceeded 40–45 °C from the oxygen isotopic composition of diagenetic minerals preserved within Early Permian strata along the flanks of the Midland basin (Bein and Land, 1983; see also Ruppel and Hovorka, 1995).

Permian sediments of the Anadarko Basin were deposited as a thin mantle of regionally derived detrital muds and sands from the Wichita and Arbuckle Mountains (Donovan, 1986). Although Permian strata may have been buried to a depth up to 1500 m in the center of the Anadarko basin (Johnson et al., 2001), maximum burial depths along the southern rim of the basin are considerably less as a result of depositional onlapping against the Wichita highlands throughout post-Pennsylvanian time. For example, the Permian strata in the Slick Hills area, just north of the Wichita

Mountains (Fig. 1), were never buried under more than a few hundred meters of post-Permian sediments (Donovan et al., 2001).

Pedogenically modified horizons comprise a major stratigraphic component of the Permo–Pennsylvanian overbank deposits in both basins. The paleosols preserve a broad range of macro- and micromorphological soil features, including angular blocky peds, argillans, slickensides, sepic–plasmic microstructure, root moulds and rhizoliths. Tabor and Montañez (2004) identified eight distinctly different groups of paleosols, or pedotypes (Retallack, 1994), that formed across the Permo–Pennsylvanian landscape of the study area. Detailed descriptions, mineralogic and chemical analyses of the various paleosols are given elsewhere (Tabor et al., 2002; Tabor and Montañez, 2004). Below, we summarize the pedogenic characteristics of these paleosols from which samples were analyzed for this study (see also Tables 1–3).

Fifteen phyllosilicate samples were taken from fifteen different paleosol profiles characterized by six distinctly different paleosol morphologies. Using the classification of Mack et al. (1993), these paleosol morphologies are Argillisols (1 to–3, and 349,941; Table 3), Calcic Argillisols (5, 6, 8 and Waur4A), Vertisols (MM3C), Calcic Vertisols (4, 7, 11, 12), and Calcisols (9 and 10). The Argillisols show evidence of illuvial concentrations of clay in the form of clay skins, or cutans, in their subsurface horizons and likely formed under relatively well-drained conditions (Soil Survey Staff, 1975). Calcic Argillisols also show evidence for subsurface illuvial concentration of clay-size material, but preserve a basal horizon with millimeter (mm)- to centimeter (cm)-scale carbonate nodules and rhizoliths. These profiles likely formed under well-drained conditions in a climate characterized by seasonal precipitation (Tabor and Montañez, 2004; Soil Survey Staff, 1975). Vertisols preserve wedge-shape aggregate structure, slickensides and clastic dikes that were apparently generated from shrink–swell processes in a seasonal moisture regime, the drainage of which was at least intermittently poor. Calcic Vertisols share similar morphological characteristics to Vertisols, but also have calcareous nodules and rhizoliths distributed throughout the paleosol matrix. The dominant feature of Calcisols is preservation of calcareous nodules and rhizoliths in subsurface horizons. These carbonates presumably formed in

Table 2
Calculated chemical formulae for end-member 2 : 1 phyllosilicate

Sample	Chemical formula[+]
Texas	
12	$(Na_{0.31}K_{0.38})(Fe_{0.26}Mg_{0.34}Al_{1.46})(Al_{0.63}Si_{3.37})O_{10}(OH)_2$*
11	$(Na_{0.55}K_{0.15})(Ti_{0.03}Fe_{0.28}Mg_{0.37}Al_{1.38})(Al_{0.51}Si_{3.49})O_{10}(OH)_2$*
10	$(Na_{0.70}K_{0.06})(Ti_{0.02}Fe_{0.22}Mg_{0.33}Al_{1.47})(Al_{0.60}Si_{3.34})O_{10}(OH)_2$*
9	$(Na_{0.33}K_{0.24})(Ti_{0.02}Fe_{0.24}Mg_{0.26}Al_{1.56})(Al_{0.59}Si_{3.41})O_{10}(OH)_2$*
8	$(Na_{0.36}K_{0.24})(Fe_{0.27}Mg_{0.39}Al_{1.43})(Al_{0.50}Si_{3.50})O_{10}(OH)_2$*
7	$(Na_{0.30}K_{0.18})(Ti_{0.04}Fe_{0.38}Mg_{0.26}Al_{1.37})(Al_{0.41}Si_{3.59})O_{10}(OH)_2$*
6	$(Na_{0.36}K_{0.30})(Ti_{0.03}Fe_{0.28}Mg_{0.25}Al_{1.50})(Al_{0.62}Si_{3.38})O_{10}(OH)_2$*
5	$(Na_{0.36}K_{0.28})(Ti_{0.04.24}Mg_{0.24}Al_{1.54})(Al_{0.63}Si_{3.37})O_{10}(OH)_2$*
4	$(Na_{0.81}K_{0.06})(Ti_{0.02}Fe_{0.17}Mg_{0.17}Al_{1.60})(Al_{0.61}Si_{3.39})O_{10}(OH)_2$*
3	$(Na_{0.22}K_{0.39})(Fe_{0.23}Mg_{0.31}Al_{1.54})(Al_{0.54}Si_{3.46})O_{10}(OH)_2$*
MM3C	$(Na_{0.23}K_{0.55})(Ti_{0.07}Fe_{0.58}Mg_{0.40}Al_{1.04})(Al_{0.68}Si_{3.32})O_{10}(OH)_2$*
1	$(Ca_{0.01}Na_{0.19}K_{0.31})(Ti_{0.11}Fe_{0.21}Mg_{0.13}Al_{1.56})(Al_{0.51}Si_{3.49})O_{10}(OH)_2$*
Oklahoma	
349941	$(Na_{0.06}K_{0.28})(Ti_{0.02}Fe_{0.28}Mg_{0.32}Al_{1.58})(Al_{0.65}Si_{3.35})O_{10}(OH)_2$*
Waur4A	$(Na_{0.03}K_{0.20})(Ti_{0.03}Mg_{0.26}Fe_{0.26}Al_{1.63})(Al_{0.53}Si_{3.47})O_{10}(OH)_2$*

*Calculated 2 : 1 phyllosilicate end-member chemical formulas for mixed 2 : 1 and 1 : 1 minerals in the Permo–Pennsylvanian <0.2 μm size fractions. See text for discussion. The chemical formulas were calculated based on 12 oxygen and 2 hydrogen atoms present in each unit-cell (Moore and Reynolds, 1997), from the oxide data reported in Table 1. The analytical uncertainty for the molar concentrations of the different elemental constituents is less then ±0.02 from the reported value.

[+] A chemical formula for end-member 2 : 1 phyllosilicate in the SS10 < 0.2 μm size fraction was not calculated, as the this sample is analytically indistinguishable from pure kaolinite.

Table 3
Measured isotope compositions, oxygen and hydrogen isotope fractionation factors and estimated temperature of phyllosilicate formation

Sample	Pedotype	$\delta^{18}O_{SMOW} \pm 0.2‰$	$\delta D \pm 4‰$	Kaolin† (wt.%)	$10^3 \ln\alpha^{18}_{2:1-H_2O}$ [1]	$10^3 \ln\alpha^{D}_{2:1-H_2O}$ [2] $= -2.2*10^6*T^{-2}+$	$10^3 \ln\alpha^{18}_{sample-H_2O}$ [3]	$10^3 \ln\alpha^{D}_{sample-H_2O}$ [4] $= -2.2*10^6*T^{-2}+$	°C [5] (±3°)	Surface domain	$\delta^{18}O_{SMOW}$ meteoricwater [6]
Texas											
12	Calcic Vertisol	22.0	−62	9	$2.83*10^6*T^{-2}-4.88$	−15.00	$2.82*10^6*T^{-2}-5.06 \pm 0.06$	-13.32 ± 0.47	27	MSD	−4.2
11	Calcic Vertisol	22.6	−62	1	$2.83*10^6*T^{-2}-4.71$	−16.29	$2.83*10^6*T^{-2}-4.73 \pm 0.05$	-16.04 ± 0.70	28	MSD	−3.9
10	Calcisol	22.7	−57	3	$2.83*10^6*T^{-2}-4.71$	−14.60	$2.83*10^6*T^{-2}-4.78 \pm 0.07$	-14.02 ± 0.55	29	MSD	−3.5
9	Calcisol	21.2	−58	1	$2.85*10^6*T^{-2}-4.83$	−14.77	$2.85*10^6*T^{-2}-4.85 \pm 0.05$	-14.56 ± 0.62	34	WESD	−4.2
8	Calcic Argillisol	21.8	−66	5	$2.83*10^6*T^{-2}-4.94$	−15.85	$2.83*10^6*T^{-2}-5.04 \pm 0.06$	-14.74 ± 0.60	26	MSD	−4.8
7	Calcic Vertisol	21.1	−61	13	$2.83*10^6*T^{-2}-4.71$	−19.70	$2.82*10^6*T^{-2}-5.00 \pm 0.07$	-15.99 ± 0.67	33	MSD	−4.0
6	Caclic Argillisol	21.1	−59	11	$2.84*10^6*T^{-2}-4.90$	−16.16	$2.83*10^6*T^{-2}-5.13 \pm 0.06$	-16.04 ± 0.70	34	WESD	−3.8
5	Calcic Argillisol	20.6	−61	8	$2.85*10^6*T^{-2}-4.92$	−14.95	$2.84*10^6*T^{-2}-5.08 \pm 0.06$	-11.03 ± 0.29	35	WESD	−4.2
4	Calcic Vertisol	20.8	−69	2	$2.88*10^6*T^{-2}-4.83$	−12.57	$2.88*10^6*T^{-2}-4.87 \pm 0.06$	-12.29 ± 0.40	31	MSD	−5.5
3	Argillisol	19.5	−66	18	$2.85*10^6*T^{-2}-4.86$	−14.36	$2.83*10^6*T^{-2}-5.23 \pm 0.06$	-11.71 ± 0.33	34	WESD	−5.3
MM3C	Vertisol	19.6	−66	44	$2.88*10^6*T^{-2}-5.70$	−23.79	$2.83*10^6*T^{-2}-6.20 \pm 0.03$	-12.34 ± 0.41	33	MSD	−4.4
2	Argillisol	19.6	−60	97			$2.76*10^6*T^{-2}-6.75 \pm 0.03$	-7.70 ± 0.70	24	MSD	−4.9
1	Argillisol	20.4	−68	65	$2.85*10^6*T^{-2}-4.79$	−14.33	$2.78*10^6*T^{-2}-6.11 \pm 0.06$	-8.72 ± 0.12	22	MSD	−5.4
Oklahoma											
349941	Argillisol	20.4	−55	29	$2.82*10^6*T^{-2}-4.95$	−15.99	$2.80*10^6*T^{-2}-5.57 \pm 0.06$	-11.44 ± 0.37	33	MSD	−3.9
Waur4A	Calcic Argillisol	21.4	−60	18	$2.83*10^6*T^{-2}-4.76$	−15.25	$2.82*10^6*T^{-2}-5.15 \pm 0.06$	-12.29 ± 0.37	30	MSD	−4.1

*Detailed descriptions of morphological characteristics, stratigraphic occurrence and distribution of paleosol types is given in Tabor and Montañez (2004).

†Estimated wt.% kaolinite in mixed 2:1 and 1:1 phyllosilicate samples as calculated from FTIR-data. The error in this estimate is ±3% of the reported value. See text for discussion.

[1] Calculated oxygen isotope fractionation factors between 2:1 phyllosilicate present in the Permo–Pennsylvanian <0.2 μm size fractions and water. Fractionation factors were calculated using the bond-model data of Savin and Lee (1988) in conjunction with the calculated chemical composition for the end-member 2:1 phyllosilicates presented in Table 2. Analytical uncertainties for these fractionation factors, resulting from uncertainties of the calculated 2:1 phyllosilicate chemical composition, do not change the reported values at the level of significance presented here. See text for discussion.

[2] Calculated hydrogen isotope fractionations between 2:1 phyllosilicate present in the Permo–Pennsylvanian <0.2 μm size fractions and water. Fractionation factors were calculated based on the molar fraction of elements in the octahedral layer as proposed by Gilg and Sheppard (1995). See text for discussion.

[3] Calculated oxygen isotope fractionation factors between mixed phyllosilicate mineralogies from the Permo–Pennsylvanian <0.2 μm size fractions and water. Fractionation factors were calculated based on the molar fraction of oxygen contributed from smectite and kaolinite in each sample. The reported errors reflect the uncertainty (±3%) of 2:1 and 1:1 phyllosilicate concentration within samples. See text for discussion.

[4] Calculated hydrogen isotope fractionation factors mixed phyllosilicate mineralogies from the Permo–Pennsylvanian <0.2 μm size fractions and water. Fractionation factors were calculated based on the molar fraction of hydrogen contributed from smectite and kaolinite in each sample. The reported errors reflect the uncertainty (±3%) of 2:1 and 1:1 phyllosilicate concentration within samples. See text for discussion.

[5] Calculated temperatures in degrees Celsius for each phyllosilicate sample in equilibrium with meteoric water. The analytical uncertainty of the reported value is ±3 °C. See text for discussion.

[6] Calculated δ^{18} O of meteoric water in equilibrium with the phyllosilicate samples. See text for discussion.

environments where evaporation of moisture from the soil exceeded the ability of precipitation to leach Ca^{2+} from the soil profile. Although well-drained conditions are not prerequisite to formation of carbonate in soil, these soils are interpreted to have formed on stable, well-drained portions of the Permian landscape (Tabor and Montañez, 2004).

2. Methods

Samples were initially collected in aluminum foil or canvas bags from the most clay-rich horizons in the soil profiles. Approximately 500 g of bulk paleosol matrix was dispersed in deionized water and shaken overnight. An aliquot of the <2 μm size fraction from the samples was collected by centrifugation. The remaining <2 μm size fraction was further reduced by centrifugation to isolate only the <0.2 μm-size fraction because this fraction is dominated by pedogenic clays (Stern et al., 1997; Tabor et al., 2002; Vitali et al., 2002). Samples were subsequently treated by a series of selective dissolution procedures to remove non-phyllosilicate constituents that may complicate interpretation of $\delta^{18}O$ values. Chemical pretreatments follow in the order of application: (1) 0.5 M NaAOc to remove calcite (Savin and Epstein, 1970, Lawrence and Taylor, 1971), (2) 30% H_2O_2 solution to remove organic matter, and (3) Sodium citrate–bicarbonate–dithionite solution (80 °C) to remove admixed secondary iron oxy-hydroxides (Jackson, 1979).

The resulting phyllosilicate clays were exchange-saturated with K or Mg on filter membranes and transferred to glass slides as oriented aggregates for X-ray diffraction analysis. Duplicate Mg-saturated clays were also prepared with glycerol. Oriented aggregates of all Mg-treated samples were analyzed without heating, at room temperature (~24 °C); the K-treated samples were analyzed without heating and after heating at 300 and 500 °C for 2 hours. Step scan analyses were performed in the Department of Land, Air and Water Resources, UC Davis on a Diano 8500 X-ray diffractometer using CuKα radiation between 2° and 30° 2θ with a step size of 0.02° 2θ and count time of 2 s. Mineralogic composition of the samples was determined following the methods of Moore and Reynolds (1997).

It is important to note that all of the phyllosilicate samples so analyzed were stored in a 2 M NaCl solution and subsequently washed to remove excess NaCl before chemical analysis. Samples were subsequently split into four aliquots for chemical analysis. The first of these three aliquots was fused into glass at high temperature (~1200 °C) upon a molybdenum strip in an Ar atmosphere. The glasses were analyzed for major and minor elemental compositions using a Cameca SX 50 microprobe in the Department of Geology, UC Davis. The majority of exchange sites in these phyllosilicates should thus be occupied by Na^+, which should be reflected in the elemental chemical data.

The second aliquot of the <0.2 μm-size fraction was analyzed for $\delta^{18}O$ following reaction with BrF_5 at ~560 °C (Clayton and Mayeda, 1963), on a Finigan MAT 252 isotope ratio mass spectrometer in the Dept. of Geology, Southern Methodist University (SMU). Repeated oxygen isotope analyses of NBS-29 yielded an analytical uncertainty of ±0.2‰. The third aliquot was analyzed for hydrogen isotope composition following the methods of Savin and Epstein (1970). Samples were initially outgassed at 250 °C in vaccuo to remove sorbed and interlayer waters and then dehydrated at a temperature of ~1000 °C. The total water extracted from the mineral was purified by distillation and quantitatively converted to H_2 by passing it over hot uranium at ~800 °C. The isotopic composition of the hydrogen gas was analyzed on a Finigan MAT 252 isotope ratio mass spectrometer in the Dept. of Geology, SMU. Replicate analyses of samples yield an analytical uncertainty of about ±4‰. Both oxygen and hydrogen isotopic compositions are reported relative to the V-SMOW standard (Gonfiantini, 1984).

Six synthetic mixtures of kaolinite and smectite over a range of compositions including the pure end-members were prepared for Fourier Transform infrared (FTIR) analyses in order to calibrate the spectra from natural samples for their relative compositions of smectite and kaolinite. The kaolinite is China clay (Ward's Kaolinite, API#9), whereas the smectite is a "standard soil montmorillonite" (R. Southard, pers. comm. 2002). The end-member samples were initially treated with 30% H_2O_2 to remove any adsorbed organics, and were then centrifuged in distilled H_2O to collect the <0.2 μm equivalent spherical diameter (esd) size fraction of both

minerals. The <0.2 μm-size fraction was analyzed with X-ray diffraction to confirm that the mineralogy of the fine fractions were the same as the mineralogy as the bulk end-member samples. Chemical analysis of the <0.2 μm "standard soil montmorillonite" indicates that it is a dioctahedral montmorillonite [$(K_{0.01}Ca_{0.04}Na_{0.17})(Ti_{0.01}Fe_{0.16}Mg_{0.26}Al_{1.57})(Si_{4.00})(O_{10})OH_2$].

For FTIR analysis, both synthetic mixtures and natural paleosol samples were diluted for diffuse reflectance by combining 2 mg of sample with 98 mg of KBr. Five hundred spectra were collected for each sample in the spectral range of 600–4000 cm^{-1} with a resolution of 2 cm^{-1} on a Nicolet 20 SXB in the Thermochemistry Facility at the University of California, Davis.

3. Results

The mineralogic composition, determined by X-ray diffraction analysis, and the chemical composition of the phyllosilicates, determined by electron microprobe analysis, are presented in Table 1. These data indicate that all of the samples lie within the compositional range of 2:1 dioctohedral phyllosilicates such as smectite, hydroxy-interlayered minerals (HIM) and mica-like materials, the 1:1 phyllosilicate kaolinite, or a mixture of 2:1 and 1:1 phyllosilicate minerals.

Phyllosilicates in the <0.2 μm size fraction of natural samples exhibit two different crystal morphologies. One morphology occurs as tabular or sheet-like structures ranging from ~150 to 200 nm that coalesce to form agglomerated structures as large as 1000 nm across (the larger structures may form upon dessication of the <0.2 μm size fraction, Fig. 2). The second morphology is tabular particles approximately 20–50 nm across that coalesce to form framboidal agglomerations that range from 100 to ~250 nm across. It is not clear what other properties these different crystal morphologies are related to, but it may be attributed to the different mineralogies (i.e. 2:1 and 1:1 phyllosilicates) present within each sample (e.g., Wilson, 1999).

The artificial mixtures of standard phyllosilicates show a strong correlation between the band-stretching peak near 3695cm^{-1} and wt.% kaolinite, with pure kaolinite having the most prominent band-stretching peak and pure smectite the least prominent band-stretching peak. There is a good correlation between the displacement of the 3695cm^{-1} bandwidth and wt.% kaolinite (or smectite) (r^2=0.98) that is mathematically expressed as:

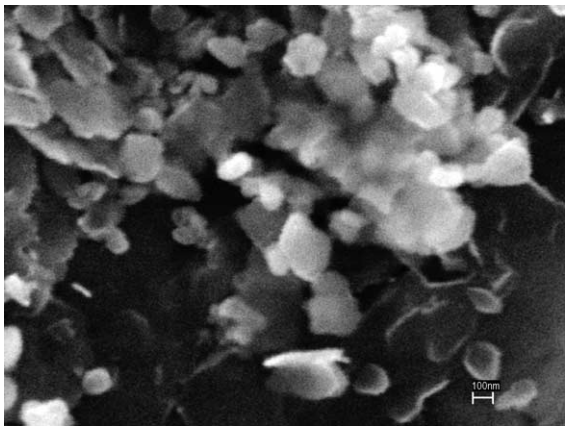

Fig. 2. Back-scatter electron image of <0.2 μm size phyllosilicate fraction from sample 8. Scale-bar is 100 nm.

$$y = 0.0045x + 0.0529,$$

where y is the negative displacement of the band-stretching peak near 3695 cm^{-1} and x is the wt.% kaolinite in the standard mixture (Fig. 3). The wt.% of kaolinite in each of the naturally occurring paleosol phyllosilicate samples is calculated using this equation. Based on the uncertainties within the calibration curve, wt.% phyllosilicate values reported in Table 2 have uncertainties of ±3%. Four samples are analytically indistinguishable from a pure 2:1 phyllosilicate, one sample is indistinguishable from a pure 1:1 kaolinite and ten samples represent some mixture of 2:1 and 1:1 minerals (Tables 1–3).

In order to estimate the chemical composition of the 2:1 phyllosilicate phases that coexist with kaolinite, it was assumed that the weight percent (wt.%) of kaolinite (which is inferred from the FTIR data) is represented as a fraction of the Al_2O_3 and SiO_2 in the measured chemical compositions (Table 1). Weight percent (wt.%)-oxide data were converted to mole fraction of Al_2O_3 and SiO_2, and the estimated aluminum and silicon contributed from kaolinite was subtracted from the natural mixtures to calculate end-member 2:1 phyllosilicate chemical formulae. These calculated phyllosilicate chemical formulae are reported in Table 2.

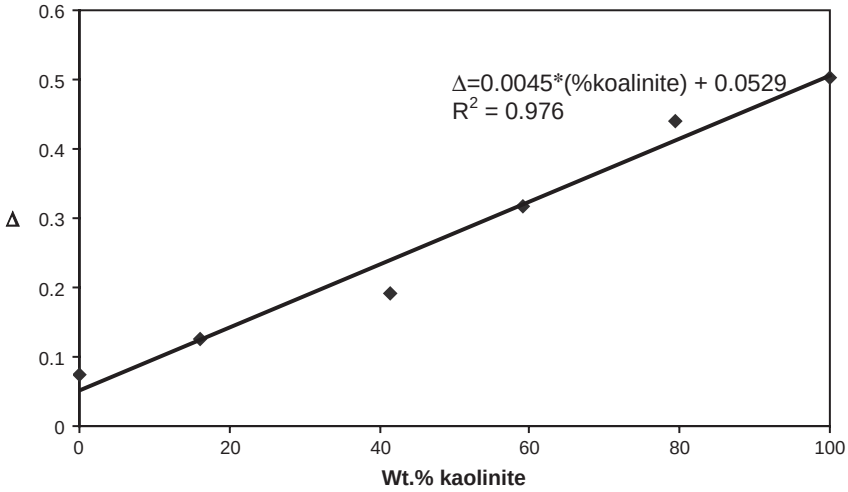

Fig. 3. Relationship between the measured peak height of the 3695cm^{-1} bandwidth and wt.% kaolinite, as measured by FTIR. Samples contain 0%, 16.2%, 41.4%, 51.9%, 79.3%, and 100% kaolinite. D values correspond to the magnitude of the adsorption spectra near 3695cm^{-1}. There is a progressive change in the peak spectra near 3695 cm^{-1} with increasing (or decreasing) percentage of kaolinite. Scatter in the relationship of peak height and wt.% kaolinite results in an uncertainty of ±3% of the reported value. See text for discussion.

Measured δD and δ^{18}O values for each of the phyllosilicate samples are presented in Table 3. The paleosol phyllosilicates exhibit a range in δD values from −69‰ to −55‰; δ^{18}O values range from 19.6‰ to 22.7‰.

4. Discussion

4.1. Stable isotopic composition of pedogenic clays as paleoenvironmental proxies

The utility of hydroxyl-bearing minerals as proxies of paleotemperature requires: (1) relatively well-known hydrogen and oxygen isotope mineral–water fractionation factors as a function of temperature; (2) isotopic equilibrium, or near equilibrium, at the time of mineral crystallization; (3) closed-system conditions for structural hydrogen and oxygen since the time of mineral formation; (4) knowledge of the relationship between hydrogen and oxygen isotope compositions of the water in the soil-forming environment and (5) water-dominated environments of crystallization. Conditions 4 and 5 have likely been constant for well-developed soils throughout the geologic past due to the processes governing the global meteoric water line and the low solubility of minerals, respectively (Yapp, 2000; Gregory, 1991). Requirements 1, 2, and 3 are specific to the mineral of interest and its paragenesis. In particular, requirement 1 is critical to drawing paleoenvironmental inferences from the stable isotope composition of phyllosilicates. This is especially true for 2:1 phyllosilicates, given their variable chemical composition and the effect of chemistry on mineral–water oxygen and hydrogen isotope fractionation (cf. Savin and Lee, 1988).

4.2. Kaolinite

Several experimentally and empirically derived oxygen isotope fractionation factors have been proposed for kaolinite, each providing significantly different values for Earth-surface temperatures (Sheppard and Gilg, 1996; and references therein). Sheppard and Gilg (1996) argued that several previously existing fractionation factors were defined using data that did not represent equilibrium values, and proposed a revised oxygen isotope fractionation equation based on pre-existing experimentally and empirically calculated data:

$$1000\ln\alpha = 2.76*10^6/T^2 - 6.75.$$

In this study, we utilize this fractionation equation for oxygen isotope fractionation in kaolinite.

Several experimentally and empiricaly derived fractionation factors have been proposed for hydrogen isotopes in kaolinite. Sheppard and Gilg (1996) proposed a hydrogen isotope fractionation factor based on a revision of existing data:

$$1000 \ln\alpha = -2.2*10^6/T^2 - 7.7.$$

This hydrogen isotope fractionation factor is used in this study given the lack of more robust hydrogen isotope fractionation factors for kaolinite.

4.3. 2:1 phyllosilicates

Low-temperature oxygen isotope fractionation factors for 2:1 phyllosilicates were proposed by Savin and Epstein (1970) and Lawrence and Taylor (1971, 1972) based on naturally occurring samples from weathering profiles, soils and sedimentary deposits. They observed a range of α-values from ~1.025 to ~1.028 for earth surface temperatures. However, these workers also recognized that the fractionation value tends to decrease with increasing Fe content, which can be quite variable in naturally occuring smectites (e.g. Table 2). The isotopic compositions of chemically characterized smectites are too few to quantify the effects of variable chemistry on the oxygen isotope fractionation between 2:1 phyllosilicates and the water from which it precipitates. Following the empirical bond-type calculations of Taylor and Epstein (1961), Savin and Lee (1988) considered that the oxygen isotope fractionation of a given phyllosilicate could be reasonably approximated by assuming that fractionation is equivalent to the weighted sum of fractionation values for the different oxygen-sharing bonds in the phyllosilicate crystal lattice. In the absence of better experimental or theoretical data, the bond-model calculation of oxygen isotope fractionation factors for 2:1 phyllosilicates is adopted in this study.

There is no generally accepted hydrogen isotope fractionation factor for 2:1 phyllosilicates. This reflects the paucity of data available for chemically characterized samples (Sheppard and Gilg, 1996). Sheppard and Gilg (1996) recognized that the fractionation of hydrogen isotopes between Al-rich, Fe-free montmorillonites and water is similar to the hydrogen isotope fractionation factor between kaolinite and water (Gilg and Sheppard, 1996), but that fractionation increases with increasing Fe-content. Furthermore, Gilg and Sheppard (1995) determined, based on the study of naturally occurring smectites, that the hydrogen isotope fractionation factor for any smectite is largely determined by the cationic composition of its octahedral layer. This is similar to the effect that was proposed by Suzuoki and Epstein (1976) for hydrogen isotope fractionation in other hydroxyl-bearing minerals:

$$1000 \ln\alpha_e = \alpha/T^2 + k,$$

where α_e is the hydrogen isotope equilibrium fractionation factor and α is the temperature dependent fractionation of some end-member component, such as Al-rich, Fe-free smectite. The constant k is determined from the molar fractions of the six-fold coordinated cations in the crystal. If the kaolinite–hydrogen isotope fractionation factor is a useful model for Fe- and Mg-free smectite minerals (cf. Gilg and Sheppard, 1996), then a reasonable hydrogen isotope fractionation factor for natural smectites of a range of chemical compositions can be calculated through the relation:

$$1000 \ln\alpha = -2.2*10^6/T^2 - 7.7 + (2\mathrm{XAl} - 4\mathrm{XMg} - 68\mathrm{XFe}),$$

where XAl, XMg, and XFe represent the molar fraction of aluminum, magnesium, and iron, respectively, in the six-fold coordinated octahedral layer of the crystal. While we recognize that this type of calculation should only be regarded as approximating the hydrogen isotope fractionation factor, we utilize this equation in the absence of superior experimental or theoretical data.

4.4. The "Illite" problem

"Illite" is a problematic term, in that this mineral is an accepted and clearly distinct mineral series name defined on the basis of the chemical composition of pure, homogeneous materials (Rieder et al., 1998). This chemical definition of illite, however, cannot be practically applied to most naturally occurring clay-sized mixtures of phyllosilicates. This reflects that in X-ray diffraction analysis of fine-clay minerals, illite is identified by basal (001) spacing of ~10 Å in

the absence of good chemical data (e.g. Jackson, 1979). Although these mica-like minerals are typically attributed to deposition as a detrital phase or diagenetic mineral in most geological studies, mica-like material may form as a result of mineralogical transformation from primary micas in soil profiles (Wilson, 1999). Furthermore, Vitali et al. (2002) and Gilg (2000), in studies of Mesozoic-age paleosols, presented compelling evidence for isotopic equilibrium of illites (i.e., degraded illites, mica-like materials or hydrous micas) with paleo-meteoric waters that may have been facilitated through transformation and dissolution processes. It is expected that the oxygen and hydrogen isotope fractionation factors will be variable for this mineral group because of the potential for different chemical compositions in "illite". In this work, we use the bond-model calculation of Savin and Lee (1988) to calculate the oxygen isotope fractionation factor and the hydrogen isotope fractionation factor adapted for this study from Gilg and Sheppard (1995) and Suzuoki and Epstein (1976) for mica-like minerals present in the phyllosilicate mixtures.

4.5. Calculated isotope fractionation factors for naturally occurring phyllosilicates

Using the bond-model approach of Savin and Lee (1988), oxygen isotope fractionation equations were calculated for the 2 : 1 phyllosilicate minerals in each sample (Table 3). In addition, hydrogen isotope fractionation equations between 2 : 1 phyllosilicates and water are calculated based on the molar fraction of the six-fold coordinated cations in the octahedral layer (Suzuoki and Epstein, 1976; Sheppard and Gilg, 1996; Table 3).

For samples that contain both kaolinite and smectite (Tables 1–3), an additional oxygen and hydrogen isotope fractionation equation was calculated based on the molar fraction of oxygen and hydrogen contributed from kaolinite and 2 : 1 phyllosilicate present in each mixture (Table 2). It is important to consider mole fraction values in these mixtures given that the differences in the contribution of hydrogen and oxygen from the 2 : 1 phyllosilicates and kaolinite are significant and not represented by a simple weight percent (wt.%) calculation (cf. Yapp, 1990).

The isotopic composition of authigenic minerals in modern soil-weathering systems (Girard et al., 2000; Yapp, 1997) and many paleosols (Yapp, 1993) indicates that isotopic equilibrium with meteoric water, or near-equilibrium values, is approached by different minerals in a soil. Assuming the conditions of isotopic equilibrium with meteoric water and retention of original isotopic compositions, Yapp (1987, 1993, 2000) and Delgado and Reyes (1996) proposed that the δD and δ^{18}O values of ancient soil-formed hydroxylated minerals might serve as single-mineral paleothermometers.

The isotopic relationship between hydrogen and oxygen in meteoric waters is well known (Craig, 1961). The mathematical expression for this relationship is:

$$\delta D_w = 8*\delta^{18}O_w + 10,$$

where the subscript "w" represents meteoric water.

Using the respective oxygen and hydrogen isotope fractionation equations of Savin and Lee (1988) and Capuano (1992), Delgado and Reyes (1996) proposed the following equation as a single-mineral geothermometer for smectite minerals that precipitate in equilibrium with meteoric waters:

$$3.54*10^6 T^{-2} = \delta^{18}O_{sm} - 0.125\delta D_{sm} + 8.95,$$

where $\delta^{18}O_{sm}$ and δD_{sm} are measured smectite δ^{18}O and δD values. In their application of this model, Delgado and Reyes (1996) did not consider the potential effects of chemical variability in the 2 : 1 phyllosilicates or the presence of co-existing kaolinite, because the samples in that study were chemically homogeneous smectites. However, in this study of Permo–Pennsylvanian paleosols, the phyllosilicate fractions are variable mixtures of 2 : 1 and 1 : 1 phyllosilicates with a range of chemical compositions (Tables 1–3). The range of calculated α values for phyllosilicate–water oxygen and hydrogen isotope fractionation (Table 3) reflects the mineralogic and chemical heterogeneity among these samples.

It is important to note that studies of modern soil profiles demonstrate that different size fractions of pedogenically formed kaolinite may have distinctly different oxygen isotope compositions, which is presumably related to different "populations" of kaolinite that formed at different times and under different environmental conditions within the same soil profile (Giral-Kacmarcik et al., 1998). This issue may also

apply to the phyllosilicates from the late Pennsylvanian and early Permian paleosols in this study. Nevertheless, the paleotemperature estimate that is made from combined oxygen and hydrogen isotope values of such a sample will provide a time-averaged value that is representative of soil-forming temperatures throughout the period of phyllosilicate formation within the soil profile so long as all of the pyllosilicate within the sample formed in oxygen and hydrogen isotope equilibrium with meteoric water (Fig. 4).

The δD and δ^{18}O values of <0.2 μm-size phyllosilicates in the Permo–Pennsylvanian paleosols range from −55‰ to −69‰ and 19.5‰ to 22.7‰, respectively (Table 3). When considered in conjunction with their respective hydrogen and oxygen isotope fractionation equations, the measured δD and δ^{18}O values indicate a temperature range for phyllosilicate crystallization of 22 to 35 ± 3 °C (Table 3). It is difficult to assess the magnitude of analytical uncertainty associated with these paleotemperature estimates. This reflects that a "propagation of errors" cannot be realistically calculated, because the uncertainty of temperature-dependent mineral–water fractionation factors for these minerals are not well known (Gilg and Sheppard, 1995; Sheppard and Gilg, 1996). However, the uncertainty in measured isotope values of the phyllosilicates indicates that paleotemperature estimates have an analytical uncertainty of ± 3 °C. In this regard, the reported paleotemperature estimates have an analytical uncertainty that is probably no better than ± 3 °C.

The isotopic composition of phyllosilicates from Permo–Pennsylvanian paleosols of Texas define a sharp rise in estimated temperatures from values of 22 ± 3 °C to 24 ± 3 °C in latest Pennsylvanian strata to values of 31 ± 3 to 34 ± 3 °C in earliest Permian strata (Fig. 5). Within the Lower Permian strata, there is a general trend toward slightly lower temperatures

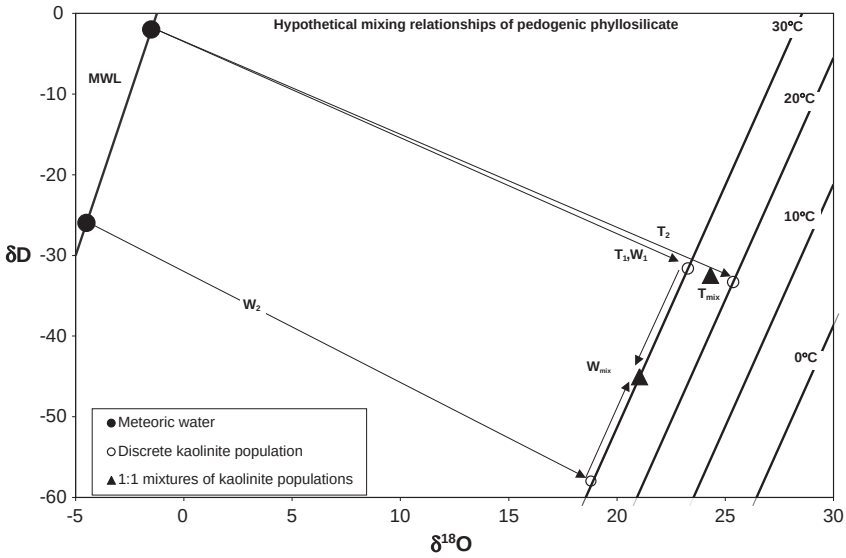

Fig. 4. Plot of δD vs. δ^{18}O values showing the meteoric water line (upper left) and 0, 10, 20 and 30 °C isotherms that represent kaolinite–meteoric water hydrogen and oxygen isotope equilibrium. The large filled circles represent hypothetical oxygen and hydrogen isotope values for soil water. The open circles represent hypothetical kaolinite populations that formed in equilibrium with soil waters at 20 or 30 °C. Arrows T_1 and T_2 point to two different kaolinite populations that formed in equilibrium with the same waters, but at different temperatures. Arrows W_1 and W_2 point to two different kaolinite populations that formed in equilibrium with different waters, but at the same temperature. For illustrative purposes, the filled triangles represent 1 : 1 mixtures of (1) kaolinite populations that formed from the same waters, but at different temperatures (T_{mix}) and (2) kaolinite populations that formed at the same temperature, but in the presence of isotopically different soil waters (W_{mix}). Note that these mixing relationships are mass balance relationships between representative populations. Therefore, if isotopically different populations of kaolinite (or smectite or smectite+kaolinite) exist within the same phyllosilicate sample, then the bulk oxygen and hydrogen isotope values, as well as the estimated temperatures of crystallization, will reflect the mass fraction of oxygen and hydrogen that is contributed from the different populations.

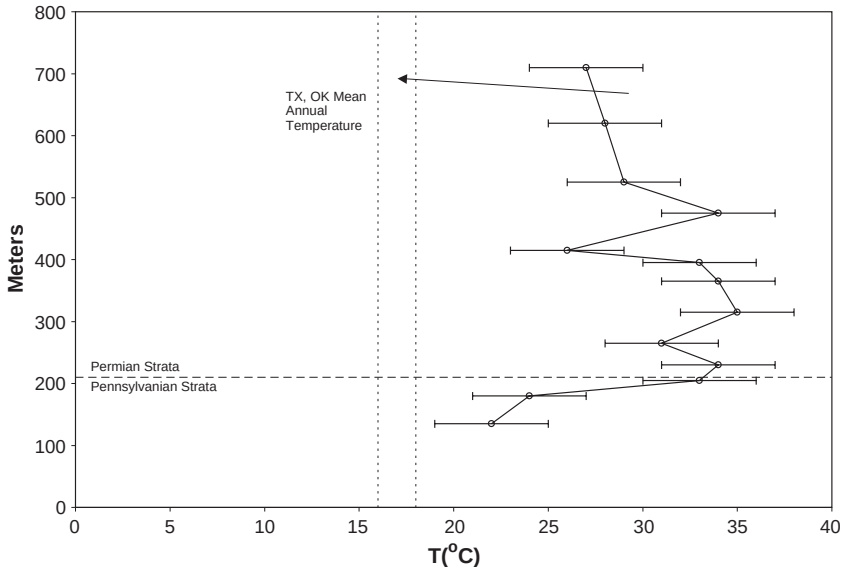

Fig. 5. Calculated temperatures (circles) of phyllosilicate samples in equilibrium with meteoric waters relative to their stratigraphic position (in meters) above the base of the late Pennsylvanian Markley Fm. The horizontal dashed line corresponds to the approximate location of the Pennsylvanian–Permian boundary in the study area. For reference, the mean annual temperature for modern north Texas and southern Oklahoma are represented by the vertical dashed line. See text.

in the upper Lower Permian. Limited biostratigraphic control and a lack of radiometric ages for these terrestrial successions limit high-resolution stratigraphic correlation between Permian strata of Oklahoma and Texas. However, temperatures estimated from the δD and δ^{18}O values of phyllosilicates in Leonardian-age paleosols from Oklahoma lie within the temperature range estimated from the Texas succession. Significantly, all of the calculated temperatures suggest crystallization of the phyllosilicates at temperatures significantly higher than modern mean annual surface air temperatures in this region (~16–17 °C).

4.6. Meteoric waters and surface domain arrays

It is known that the two most important factors to influence the δ^{18}O and δD values of naturally occurring phyllosilicates are (1) the isotopic composition of the water from which the phyllosilicates precipitate and (2) the temperature of formation. However, it is probably impossible to absolutely demonstrate that phyllosilicates from Permo–Pennsylvanian paleosols have retained their original isotope compositions or to determine whether their isotope compositions entirely reflect pedogenic conditions. Nonetheless, a global database of meteoric water δD and δ^{18}O compositions and corresponding mean annual surface air temperatures, in conjunction with oxygen and hydrogen isotope fractionation factors for a given mineral, will result in an array of isotope compositions that reflects the vast majority of possible oxygen and hydrogen isotope compositions expected for that mineral at Earth surface temperatures. Yapp (1993, 2000) applied this concept to the IAEA global precipitation database (e.g., Rozanski et al., 1993) to define a "Modern Surface Domain" (MSD) and "Warm Earth Surface Domain" (WESD) for the common low-temperature mineral goethite. Although the situation of an ancient phyllosilicate δD and δ^{18}O value within its respective MSD or WESD may not be unique to formation under such conditions, this organizing principle does provide a quantitative means to simplify the numerous factors responsible for the oxygen and hydrogen isotope composition of hydroxylated minerals (Yapp, 1993, 2000; Savin and Hsieh, 1998).

In this work, the approach used for compilation of surface domain arrays of the phyllosilicate δD and δ^{18}O data is identical to the treatment of the modern IAEA data base employed by Yapp (2000). The weighted mean δ^{18}O composition of precipitation

($\delta^{18}O_{precip}$) at each site in the IAEA database is used to calculate the δD of meteoric precipitation. This assumes that the meteoric water line (MWL) of Craig (1961) correctly represents the relationship between the δD and δ^{18}O of meteoric waters through time. In addition, only waters from IAEA sites with a mean annual temperature >0 °C are used to construct the MSD as it is expected that liquid water is a requirement for crystallization of hydroxylated minerals. This treatment of the IAEA database yields 184 data points (Rozanski et al., 1993), ranging from 0 to ~30 °C. When considering these modern IAEA data in conjunction with oxygen and hydrogen isotope fractionation factors for a given mineralogy, there is a resulting array of estimated mineral δD and δ^{18}O values that define a MSD (e.g. Fig. 6A). These surface

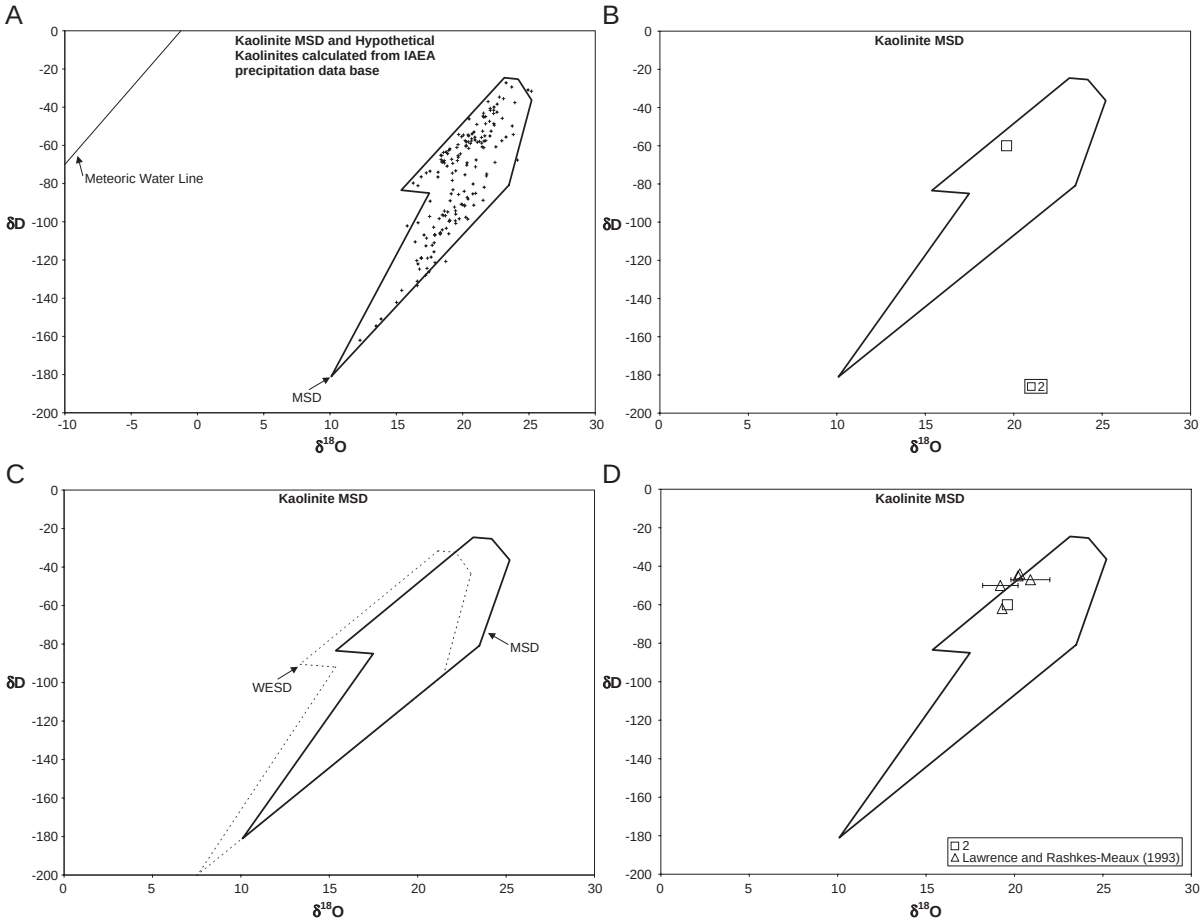

Fig. 6. (A) Plot of δD vs. δ^{18}O showing the meteoric water line (upper left) and 184 fictive kaolinite samples (crosses) that were calculated using hydrogen and oxygen isotope fractionation equations for kaolinite in conjunction with the δD, δ^{18}O, and temperature data from the IAEA data base (Rozanski et al., 1993). The polygon surrounding these fictive kaolinite data points represents the limits in δD vs. δ^{18}O space for the kaolinite Modern Surface Domain (MSD). See Text. (B) Plot of the kaolinite MSD along with the δD and δ^{18}O composition of phyllosilicate from sample 2, a nearly pure kaolinite sample taken from Pennsylvanian-age strata in the Eastern Midland basin of Texas. Sample 2 is situated within the MSD. See Text. (C) Plot of the kaolinite MSD (polygon represented by solid black line) and the corresponding kaolinite Warm Earth Surface Domain (WESD) for global temperatures that are 5 °C warmer and an ice-free Earth. See text for details and discussion. (D) Plot of the kaolnite MSD along with the δD and δ^{18}O composition of phyllosilicate sample 2 and five other nearly pure Pennsylvanian-age kaolinite samples from Texas and Missouri. The five other samples are taken from Lawrence and Rashkes-Meaux (1993). Within analytical uncertainty, all of the samples plot within the kaolinite MSD. See text for discussion.

domain arrays may be useful in determining whether the Permo–Pennsylvanian phyllosilicates preserve isotopic compositions consistent with formation at modern earth-surface conditions (e.g. Savin and Hsieh, 1998).

Fig. 6B shows the calculated MSD for kaolinite. Also shown is the δD and δ^{18}O value for sample 2 (Tables 1–3), a nearly pure kaolinite from the Late Pennsylvanian succession of Texas. The oxygen and hydrogen isotope values of this kaolinite sample plot within the MSD, suggesting that the isotopic compositions of this sample are consistent with formation in a low temperature, supergene-weathering environment. However, this MSD model is based on the measured isotopic compositions of the phyllosilicates, and gives no consideration to mode of occurrence (i.e., pedogenic in origin).

Considering the isotopic composition and the calculated oxygen and hydrogen isotope fractionation equations for each of the Permo–Pennsylvanian phyllosilicate samples (Table 3), 12 of the 15 samples plot within or upon the limits of their respective MSD. The other three samples plot just to the left of the MSD, which corresponds to an isotopic composition that may reflect phyllosilicate crystallization at slightly higher temperatures (>30 °C) than those observed on modern Earth (Table 3).

Yapp (2000) considered the consequences of a warmer Earth on the limits of surface domain arrays in δD vs. δ^{18}O space. In the Warm Earth Surface Domain (WESD) model, it is assumed that global temperatures are 5 °C warmer and that the Earth is ice-free. This concept of the WESD array may be appropriate for some of the Permian-age phyllosilicate samples, as the final episodes of Late Paleozoic deglaciation occurred within the Early Permian (Isbell et al., 2003). Using kaolinite as an example, the resultant WESD is plotted along with the MSD (Fig. 5C). The WESD is somewhat more inclusive of phyllosilicate samples with lower δ^{18}O and δD compositions than its corresponding MSD. The three phyllosilicate samples from Permo–Pennsylvanian paleosols that do not plot within the MSD lie within the WESD (Table 3).

Documenting whether an ancient mineral has preserved its original isotopic composition is very challenging. We interpret the measured isotope values of these phyllosilicates and the estimated paleotemperatures to reflect Permo–Pennsylvanian pedogenic conditions for the following reasons. First, the samples are derived from paleosols with an assemblage of minerals indicative of pedogenesis (Tabor et al., 2002). Secondly, both the Texas and Oklahoma successions have undergone a low-temperature diagenetic history. Thirdly, the phyllosilicate samples preserve isotopic compositions that are permissive of formation at Earth-surface conditions, and all samples have similar isotopic compositions that correspond to formation at temperatures well above modern temperatures in the study area. Lastly, the Upper Pennsylvanian and Lower Permian successions were deposited within the equatorial belt of the Pangean supercontinent. Therefore, if phyllosilicates from paleosols from the Midaland and Anadarko basins preserve an isotopic record of Permo–Pennsylvanian pedogenesis, it might be expected that their oxygen and hydrogen isotope compositions correspond to formation at temperatures that are characteristic of equatorial latitudes. Mean annual temperatures within modern tropical latitudes range from ~25–30 °C (e.g., Rozanski et al., 1993). Phyllosilicates from the Permo–Pennsylvanian paleosols of Texas and Oklahoma preserve isotope compositions suggesting formation over a range of temperatures that overlaps with temperatures in modern equatorial environments. Collectively, we consider these factors as persuasive evidence for preservation of original phyllosilicate oxygen and hydrogen isotope compositions that reflect Permo–Pennsylvanian pedogenesis.

There are few independently derived paleotemperature estimates for Permo–Pennsylvanian tropical latitudes to compare with paleotemperature estimates presented here. However, atmospheric pCO_2 likely increased from relatively low concentrations during late Pennsylvanian time to concentrations of 1 to 4 times modern values during early Permian time (Ekart et al., 1999; Royer et al., 2004; Tabor and Montañez 2004). Increased pCO_2 concentration during Permian time may have facilitated higher temperatures at tropical latitudes (Barron and Moore, 1994). This pattern of higher temperatures is observed in the calculated temperatures from the Texas Permo–Pennsylvanian phyllosilicate samples (Fig. 5, Table 3). Furthermore, energy balance models (Gibbs et al., 2002) that consider the effects of

elevated atmospheric pCO_2 levels on land surface temperatures indicate that tropical early Permian mean annual temperatures could have been between 25 and 35 °C. These modeled temperatures encompass the range of calculated temperatures derived from δD and δ^{18}O values of the phyllosilicate samples from western equatorial Pangea (Table 3; Fig. 5).

Previously published δD and δ^{18}O values for Pennsylvanian-age, nearly pure kaolinites from terrestrial successions in Texas and Missouri that were deposited in the equatorial region of Pangea (Lawrence and Rashkes-Meaux, 1993) have isotopic compositions similar to those in this study (Fig. 6D). Within analytical uncertainty, these samples plot within the modern surface domain and have a similar calculated range of temperatures (23–33 °C) to contemporaneous samples in this study. Collectively, these earlier studies and this work are encouraging, as they suggest that pedogenically-formed phyllosilicates may provide a reasonable proxy of terrestrial paleotemperatures.

4.7. Refinement of the Texas Permian calcite δ^{18}O record

Temperatures calculated from the Permo–Pennsylvanian phyllosilicate δ^{18}O values may be used in conjunction with their respective oxygen isotope fractionation equations to provide an independent estimate of the oxygen isotopic composition of the meteoric waters from which these samples formed (cf. Delgado and Reyes, 1996). These calculated meteoric water δ^{18}O values range from -3.5 ± 0.1 to -5.5 ± 0.1‰ (Table 3; Fig. 7). This relatively narrow range of values falls well within the range observed in modern, low-altitude equatorial sites (Rozanski et al., 1993). These estimated meteoric water δ^{18}O values may provide further understanding of other pedogenic minerals that co-exist with the phyllosilcate samples in the Permo–Pennsylvanian profiles.

Tabor et al. (2002) noted that δ^{18}O values of pedogenic calcites and phyllosilicates coexisting within individual Permo–Pennsylvanian paleosol pro-

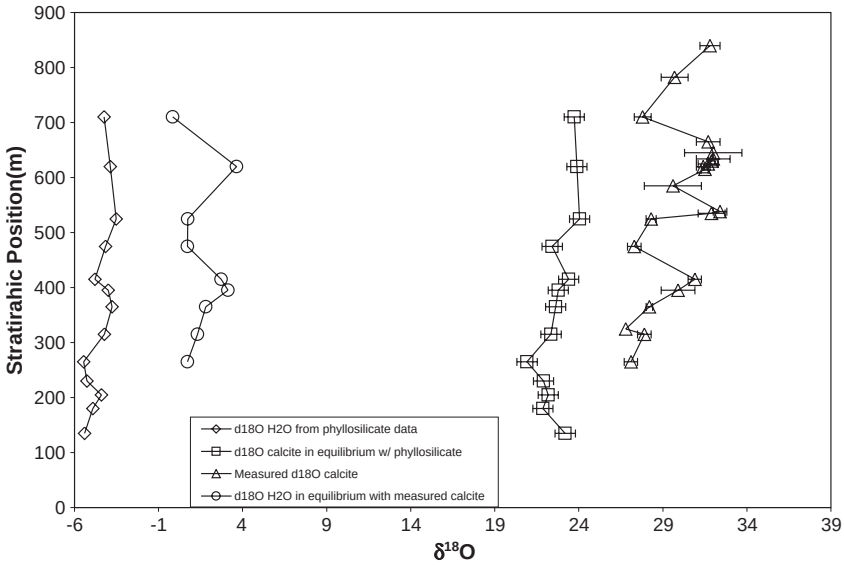

Fig. 7. Plot of the stratigraphic position (in meters) versus the calculated meteoric water δ^{18}O in equilibrium with Permo–Pennsylvanian phyllosilicates from the Eastern Midland basin (diamonds), the calculated δ^{18}O value of coexisting calcite if it formed in equilibrium with the same meteoric waters associated with the phyllosilicate samples (squares), the measured δ^{18}O values for the calcites in the Permian strata of the Eastern Midland basin (Triangles; Tabor et al., 2002) and the isotopic composition of soil water that would have formed in equilibrium with the measured calcite δ^{18}O compositions (circles) if they formed at the same temperature calculated from coexisting phyllosilicate samples. In every instance, the measured isotopic composition of the calcites indicate that these minerals apparently precipitated from water with a significantly more positive δ^{18}O value than waters associated with the phyllosilicate samples. This may be the result of isotopic modification of soil moisture from evapotranspiration prior to and during calcite formation. See text.

files did not appear to be in isotopic equilibrium with each other. This oxygen isotope disequilibrium was attributed to (1) evaporative enrichment of soil waters prior to and during calcite precipitation and/or (2) the presence of some detrital component within the phyllosilicate samples. Based on the arguments provided in this work, a detrital component is not considered to be significant in the samples analyzed here. Isotopic enrichment may be facilitated through evaporation of local soil waters. Furthermore, net evapotranspiration from the soil must exceed net precipitation passing through the soil in order for pedogenic carbonate to precipitate (e.g., Buol et al., 1997). Isotope enrichment of soil waters from evaporation does not likely apply to formation of most phyllosilicates, as these minerals require large flux of H_2O through the profile in order to facilitate mobility of Al and Si cations.

Using the oxygen isotope fractionation equation between calcite and water (O'Neil et al., 1969) and the paleotemperature and meteoric water $\delta^{18}O$ values calculated from the phyllosilicate data (Table 3), the isotopic composition of pedogenic calcite in equilibrium with the Permo–Pennsylvanian phyllosilicates was calculated (Fig. 6). In every instance, the calculated calcite $\delta^{18}O$ value is significantly lower than the measured calcite $\delta^{18}O$ value (Fig. 7). This is reflected in calculated $\delta^{18}O$ values of soil waters in equilibrium with the measured calcite $\delta^{18}O$ values that are 4.1–7.5‰ higher than the $\delta^{18}O$ values of water in equilibrium with coexisting phyllosilicate. Note that calcite $\delta^{18}O$ values have been calculated for all paleosol profiles where phyllosilicate data has been collected, but soil water $\delta^{18}O$ values in equilibrium with the measured calcite $\delta^{18}O$ compositions have been calculated only for paleosol profiles with data from phyllosilicates and calcite. Although variable pH at the time of calcite formation may have been a contributing factor to the extent of measured calcite ^{18}O enrichment over that of the calculated equilibrium values (Zeebe, 2001), these data seem to confirm the notion that evapotranspiration plays an important role in modifying the isotopic composition of soil water (and the pH of soil moisture; Cerling and Quade, 1993) across the Permian equatorial landscape. Thus, the $\delta^{18}O$ composition of ancient soil carbonate minerals likely provides an indication of paleo-soil water $\delta^{18}O$ compositions modified by evaporative enrichment. Therefore, pedogenic calcite $\delta^{18}O$ values do not likely provide a faithful proxy of paleoprecipitation $\delta^{18}O$ values or robust paleotemperature estimate (cf. Nort et al., 2003).

5. Conclusions

Phyllosilicates collected from Permo–Pennsylvanian paleosol profiles of the Eastern Midland basin of Texas and Southern Anadarko basin of Oklahoma consist of 2:1 phyllosilicates and kaolinite, with 97 ± 3 to $0 \pm 3\%$ kaolinite in the mixed clay fractions. Using the chemical and mineralogic compositions of the naturally occurring phyllosilicates, oxygen and hydrogen isotope fractionation equations were calculated from previously published thermodynamic data. Assuming that these phyllosilicate samples formed in equilibrium with meteoric water, the oxygen and hydrogen isotopic composition of the samples indicate a range of formation temperatures from 22 ± 3 to 35 ± 3 °C. In particular, Permo–Pennsylvanian data from the Eastern Midland basin indicate an abrupt increase in near surface air temperatures of up to ~10 °C across the Permo–Pennsylvanian boundary. Calculated temperatures from Permian samples in the Anadarko basin fall within the range of temperatures calculated for penecontemporaneous phyllosilicate samples in the Eastern Midland basin as would be expected if these minerals preserve near-surface, pedogenic conditions. In addition, previously published δD and $\delta^{18}O$ values for Pennsylvanian-age nearly pure kaolinites from Texas and Missouri have calculated temperatures that overlap those of contemporaneous phyllosilicates presented in this work. Furthermore, the oxygen and hydrogen isotope compositions of the studied samples fall within a Modern Surface Domain array or a Warm Earth Surface Domain array, indicating that the phyllosilicate samples likely retain an isotopic record of Permo–Pennsylvanian Earth-surface conditions in western equatorial Pangea.

If the analyzed phyllosilicate samples formed in isotopic equilibrium with Permo–Pennsylvanian meteoric water, then meteoric water $\delta^{18}O$ values ranged from -5.5‰ to -3.5‰. Within the context of previously published calcite $\delta^{18}O$ values from the Eastern Midland basin (Tabor et al., 2002), the relatively narrow range of calculated meteoric water $\delta^{18}O$

values and estimated paleotemperatures indicate that calcites coexisting with phyllosilicates apparently formed from soil moisture with an isotopic composition that was significantly modified by evaporation.

Acknowledgements

We are deeply indebted to Bill Dimichele and Dan Chaney, Dept. of Paleobiology, Smithsonian Institution, for providing an introduction to the study area and a stratigraphic and paleoecologic framework in the American Southwest. We thank four anonymous reviewers, and especially Dr. Samuel Savin, for helpful comments that considerably improved the quality of this manuscript. Thanks also to Crayton Yapp for helpful and thoughtful conversations about this work. This research received support from an NSF IGERT "Nanomaterials in the Environment, Agriculture, and Technology", in addition to Grants-in-Aid to N. Tabor from the Geological Society of America, American Association of Petroleum Geologists, Society for Sedimentary Geology (SEPM) and Sigma Xi, as well as NSF grant EAR-9814640 to I.P. Montañez.

References

Barnes, V.E., Hentz, T.F., Brown Jr., L.F., 1987. Geologic Atlas of Texas; Wichita Falls-Lawton Sheet. University of Texas at Austin, Bureau of Economic Geology.

Barron, E.J., Moore, G.T., 1994. Climate model application in paleoenvironmental analysis. Society of Sedimentary Geology 33 (Short Course).

Bein, A., Land, L., 1983. Carbonate sedimentation and diagenesis associated with Mg–Ca-chloride brines; the Permian San Andres formation in the Texas panhandle. Journal of Sedimentary Petrology 53, 243–260.

Bird, M.I., Chivas, A.R., 1988. Stable-isotope evidence for low-temperature kaolinitic weathering and post-formational hydrogen-isotope exchange in Permian kaolinites. Chemical Geology 72, 249–265.

Bird, M.I., Chivas, A.R., 1989. Stable isotope geochronology of the Australian regolith. Geochimica et Cosmochimica Acta 53, 3239–3256.

Buol, S.W., Hole, F.D., McCracken, R.J., Southard, R.J., 1997. Soil Genesis and Classification. Iowa State University Press, Ames, IA. 527 pp.

Capuano, R.M., 1992. The temperature dependence of hydrogen isotope fractionation between clay minerals and water; evidence from a geopressured system. Geochimica et Cosmochimica Acta 56, 2547–2554.

Cerling, T.E., Quade, J., 1993. Stable carbon and oxygen isotopes in soil carbonates. In: Swart, P.K., Lohmann, K.C., McKenzie, J., Savin, S. (Eds.), Climate Change in Continental Isotopic Records. Geophysical Monograph, vol. 78, pp. 217–231.

Clayton, R.N., Mayeda, T.K., 1963. The use of bromine pentafluoride in the extraction of oxygen from oxides and silicates for isotopic analysis. Geochimica et Cosmochimica Acta 27, 43–52.

Craig, H., 1961. Isotopic variations in meteoric waters. Science 133, 1702–1703.

Ekart, D.D., Cerling, T.E., Montañez, I.P., Tabor, N.J., 1999. A 400 million year carbon isotope record of pedogenic carbonate: implications for paleoatmospheric carbon dioxide. American Journal of Science 299, 805–827.

Delgado, A., Reyes, E., 1996. Oxygen and hydrogen isotope compositions in clay minerals; a potential single mineral geothermometer. Geochimica et Cosmochimica Acta 60, 4285–4289.

Donovan, R.N., 1986. The geology of the Slick Hills. In: Donovan, R.N. (Ed.), The Slick Hills of Southwestern Oklahoma—Fragments of an Aulacogen?: Oklahoma Geological Survey Guidebook, vol. 24, pp. 1–12.

Donovan, R.N., Collins, K., Bridges, S., 2001. Permian sedimentation and diagenesis on the Northern Margin of the Wichita Uplift. Oklahoma Geological Survey Circular, vol. 104. University of Oklahoma Press, pp. 171–184.

Dunbar, C.O., Committee on Stratigraphy, 1960. Correlation of the Permian formations of North America. Geological Society of America Bulletin 71, 1763–1806.

Gibbs, M.T., Rees, P.M., Kutzbach, J.E., Ziegler, A.M., Behling, P.J., Rowley, D.B., 2002. Simulations of Permian climate and comparisons with climate-sensitive sediments. Journal of Geology 110, 33–55.

Gilg, H.A., 2000. D-H evidence for the timing of kaolinitization in Northeast Bavaria, Germany. Chemical Geology 170, 5–18.

Gilg, H.A., Sheppard, S.M.F., 1995. Hydrogen isotope fractionation between smectites and water. Terra Nova 7, 329.

Gilg, H.A., Sheppard, S.M.F., 1996. Hydrogen isotope fractionation between kaolinite and water revisited. Geochimica et Cosmochimica Acta 60, 529–533.

Giral-Kacmarcik, S., Savin, S.M., Nahon, D.B., Girard, J.-P., Lucas, Y., Abel, L.J., 1998. Oxygen isotope geochemistry of kaolinite in laterite-forming processes, Manaus, Amazonas, Brazil. Geochimica et Cosmochimica Acta 62, 1865–1879.

Girard, J.P., Feyssinet, P., Chazot, G., 2000. Unraveling climatic changes from intraprofile variation in oxygen and hydrogen isotopic composition of goethite and kaolinite in laterites: an integrated study from Yaou, Frech Guiana. Geochimica et Cosmochimica Acta 64, 409–426.

Gonfiantini, R., 1984. Advisory group meeting on stable isotope reference samples for geochemical and hydrological investigations. Rep Dir Gen. IAEA, Vienna.

Golonka, J., Ross, M.I., Scotese, C.R., 1994. Phanerozoic paleogeographic and paleoclimatic modeling maps. In: Embry, A.F., Beauchamp, B., Glass, D.J. (Eds.), Pangea: Global Environments and Resources. Canandian Society of Petroleum Geolologist, Memoir, vol. 17, pp. 1–47.

Gregory, R.T., 1991. Oxygen isotope history of seawater revisited: time scales for boundary event changes in the oxygen

isotope composition of seawater. In: Taylor, H.P., O'Neil, J.R., Kaplan, I.R. (Eds.), Stable Isotope Geochemistry: A Tribute to Samuel Epstein. The Geochemical Society, San Antonio, U.S.A, pp. 65–76.

Hentz, T.F., 1988. Lithostratigraphy and paleoenvironments of upper Paleozoic continental red beds, north-central–central Texas: Bowie (new) and Wichita (revised) Groups. Report of Investigations, vol. 170. The University of Texas at Austin, Bureau of Economic Geology. 49 pp.

Isbell, J.L., Lenaker, P.A., Askin, R.A., Miller, M.F., Babcock, L.E., 2003. Reevaluation of the timing and extent of late Paleozoic glaciation in Gondwana; role of the Transantarctic Mountains. Geology 31, 977–980.

Jackson, M.L., 1979. Soil Chemical Analysis—Advanced Course. Author, Madison, Wisconsin.

Johnson, K.S., Northcutt, R.A., Hinshaw, G.C., Hines, K.E., 2001. Geology and petroleum reservoirs in Pennsylvanian and Permian Rocks of Oklahoma. Oklahoma Geological Survey, Circular, vol. 104. University of Oklahoma Press, pp. 1–20.

Lawrence, J.R., Rashkes-Meaux, J.R., 1993. The stable isotopic composition of ancient kaolinites of North America. In: Swart, P.K., Lohmann, K.C., McKenzie, J., Savin, S. (Eds.), Climate Change in Continental Isotopic Records. Geophysical Monograph, 78, pp. 249–261.

Lawrence, J.R., Taylor Jr., H.P., 1971. Deuterium and oxygen-18 correlation: clay minerals and hydroxides in Quaternary soil compared to meteoric water. Geochimica et Cosmochimica Acta 35, 993–1003.

Lawrence, J.R., Taylor Jr., H.P., 1972. Hydrogen and oxygen isotope systematics in weathering profiles. Geochimica et Cosmochimica Acta 36, 1377–1393.

Loope, D.B., Steiner, M.B., Rowe, C.M., Lancaster, N., 2004. Tropical westerlies over Pangaean sand seas. Sedimentology 51, 315–322.

Mack, G.H., James, W.C., Monger, H.C., 1993. Classification of paleosols. Geological Society of America Bulletin 105, 129–136.

Moore, D.M., Reynolds, R.C., 1997. X-ray Diffraction and the Identification and Analysis of Clay Minerals. Oxford University Press, New York.

Nelson, W.J., Hook, R.W., Tabor, N., 2001. Clear Fork Group (Leonardian, Lower Permian) of North-Central Texas. Oklahoma Geological Survey, Circular 104, 167–169.

Nort, L., Atchley, S., Dworkin, S., 2003. Terrestrial evidence for two greenhouse events in the latest Cretaceous. Geological Society of America, 13.

O'Neil, J.R., Clayton, R.N., Mayeda, T.K., 1969. Oxygen isotope fractionation in divalent metal carbonates. Journal of Chemical Physics 51, 5547–5558.

Oriel, S.S., Myers, D.A., Crosby, E.J., 1967. Paleotectonic investigations of the Permian system in the United States. U.S.G.S. Professional Paper, 17–60.

Parrish, J.T., 1993. Climate of the supercontinent Pangea. Journal of Geology 101, 215–233.

Retallack, G.J., 1994. A pedotype approach to latest Cretaceous and earliest Tertiary paleosols in eastern Montana. Geological Society of America Bulletin 106, 1377–1397.

Rieder, M., Cavazzini, G., D'yakonov, Y.S., Frank-Kamenetskii, V.A., Gottardi, G., Guggenheim, S., Koval, P.V., Mueller, G., Neiva, A.M.R., Radoslovich, E.W., Robert, J.L., Sassi, F.P., Takeda, H., Weiss, Z., Wones, D.R., 1998. Nomenclature of the micas. Clays and Clay Minerals 46, 586–595.

Rozanski, K., Araguas-Araguas, L., Gonfiantini, R., 1993. Isotopic patterns in modern global precipitation. In: Swart, P.K., Lohmann, K.C., McKenzie, J., Savin, S. (Eds.), Climate Change in Continental Isotopic Records. Geophysical Monograph, vol. 78, pp. 1–36.

Royer, D.L., Berner, R.A., Montañez, I.P., Tabor, N.J., Beerling, D.J., 2004. CO_2 as a primary driver of phanerozoic climate. Geological Society of America Today, 14.

Ruppel, S.C., Hovorka, S.D., 1995. Controls on reservoir development in Devonian chert: Permian basin, Texas. American Association of Petroleum Geologist's Bulletin 79, 1757–1785.

Savin, S.M., Epstein, S., 1970. The oxygen and hydrogen isotope geochemistry of clay minerals. Geochimica et Cosmochimica Acta 34, 25–42.

Savin, S.M., Hsieh, J.C.C., 1998. The hydrogen and oxygen isotope geochemistry of pedogenic clay minerals: principles and theoretical background. Geoderma 82, 227–253.

Savin, S.M., Lee, M., 1988. Isotopic studies of phyllosilicates. In: Bailey, S.W. (Ed.), Hydrous Phyllosilicates. Reviews in Mineralogy, vol. 19, pp. 189–223.

Scotese, C.R., 1984. Paleozoic paleomagnetism and the assembly of Pangea. In: Van der Voo, R., Scotese, C.R., Bonhommet (Eds.), Plate Reconstruction From Paleozoic Paleomagnetism. Geodynamics Series Bulletin, vol. 12, pp. 1–10.

Sellwood, B.W., Price, G.D., 1993. Sedimentary facies as indicators of Mesozoic palaeoclimate. Philosophical Transactions of the Royal Society of London. Series B, Biological Sciences 341, 225–233.

Sheppard, S.M.F., Gilg, H.A., 1996. Stable isotope geochemistry of clay minerals. Clay Minerals 31, 1–24.

Soil Survey Staff, 1975. Soil taxonomy. United States Department of Agriculture, Agriculture Handbook, vol. 436. U.S. Govt. Print. Off., Washington, D.C., p. 754.

Stern, L.A., Chamberlain, P.C., Reynolds, R.C., Johnson, G.D., 1997. Oxygen isotope evidence of climate change from pedogenic clay minerals in the Himalayan molasse. Geochimica et Cosmochimica Acta 61, 731–744.

Suzuoki, T., Epstein, S., 1976. Hydrogen isotope fractionation between OH-bearing minerals and water. Geochimica et Cosmochimica Acta 40, 1229–1240.

Tabor, N.J., Montañez, I.P., 2004. Morphology and distribution of fossil soils in the Permo–Pennsylvanian Bowie and Wichita Groups, North-Central Texas, USA: their implications for western equatorial Pangean palaeoclimate during icehouse–Greenhouse transition. Sedimentology 51, 851–884.

Tabor, N.J., Montañez, I.P., Southard, R.J., 2002. Paleoenvironmental reconstruction from chemical and isotopic compositions of Permo–Pennsylvanian pedogenic minerals. Geochimica et Cosmochimica Acta 66, 3093–3107.

Taylor, H.P., Epstein, S., 1961. Relationships between $^{18}O/^{16}O$ ratios in coexisting minerals of ingneous and metamorphic

rocks: Part 2. Application to petrologic problems. Geological Society of America Bulletin 73, 675–694.

Vitali, F., Longstaffe, F.J., McCarthy, P.J., Plint, A.G., Caldwell, W.G.E., 2002. Stable isotopic investigation of clay minerals and pedogenesis in an interfluve paleosol from the Cenomanian Dunvegan Formation, N.E. British Columbia, Canada. Chemical Geology 192, 269–287.

Wilson, M.J., 1999. The origin and formation of clay minerals in soils: past, present and future perspectives. Clay Minerals 34, 7–25.

Yapp, C.J., 1987. Oxygen and hydrogen isotope variations among goethites (a-FeOOH) and the determination of paleotemperatures. Geochimica et Cosmochimica Acta 51, 355–364.

Yapp, C.J., 1990. Oxygen isotopes in Fe(III) oxides: 2. Possible constraints on the depositional environment of a Precambrian quartz–hematite banded information. Chemical Geology 85, 337–344.

Yapp, C.J., 1993. The stable isotope geochemistry of low temperature Fe(III) and Al "oxides" with implications for continental paleoclimates. In: Swart, P.K., Lohmann, K.C., McKenzie, J., Savin, S. (Eds.), Climate Change in Continental Isotopic Records. Geophysical Monograph, vol. 78, pp. 285–294.

Yapp, C.J., 1997. An assessment of isotopic equilibrium in geothites from a bog iron deposit and a lateritic regolith. Chemical Geology 135, 159–171.

Yapp, C.J., 2000. Climatic implications of surface domains in arrays of (δD and (δ^{18}O from hydroxyl minerals: geothite as an example. Geochimica et Cosmochimica Acta 64, 2009–2025.

Zeebe, R.E., 2001. Seawater pH and isotopic paleotemperatures of Cretaceous oceans. Palaeogeography, Palaeoclimatology, Palaeoecology 170, 49–57.

Ziegler, A.M., Hulver, M.L., Rowley, D.B., 1996. Permian world topography and climate. In: Martini, I.P. (Ed.), Late Glacial and Postglacial environmental changes—Quaternary, Carboniferous–Permian and Proterozoi. Oxford Univ. Press, New York.